

Robust Control of an Evaporator Through Algebraic Riccati Equations and D-K Iteration

Javier Jiménez-Cabas[1], Farid Meléndez-Pertuz[1(✉)], David Ovallos-Gazabon[2], Jaime Vélez-Zapata[1], Hermes E. Castellanos[3], César A. Cárdenas[3], Joaquín F. Sánchez[3], Gonzalo Jimenez[3], César Mora[4], Fredy A. Sanz[3], and C. A. Collazos[3]

[1] Departamento de Ciencias de la Computación y Electrónica, Universidad de la Costa, Barranquilla, Colombia
fmelendel@cuc.edu.co
[2] Departamento de Ingeniería de procesos Industriales, Institución Universitaria ITSA, Barranquilla, Colombia
[3] Vicerrectoría de Investigaciones, Universidad Manuela Beltrán, Bogotá, Colombia
[4] Centro de Investigación en Ciencia Aplicada y Tecnología Avanzada del Instituto Politécnico Nacional, México DF, Mexico

Abstract. Evaporation is a process that is widely used in the chemical industry and aims to concentrate a solution consisting of a non-volatile solute and a volatile solvent. In this paper the design of robust control systems for a simple effect evaporation system is presented. Two controllers were designed, the first was based on the Algebraic Riccati Equations (ARE) solutions technique and the second was derived from the D-K iteration method. To show the potentiality of the control system proposed, we present the results of some tests carried out in simulation.

Keywords: Robust control · Single effect evaporator · Algebraic Riccati equations · D-K iteration

1 Introduction

Evaporation is a technique widely used in industrial chemical processes and aims to concentrate a solution consisting of a non-volatile solute and a volatile solvent. Water is normally used as a solvent and the process consists in evaporating some of it in order to achieve the concentrated solution. Despite frequent use the various applications of evaporation processes in industry, it has been found that the control strategies currently used on these systems do not offer the best performance [1–3]. For this reason, it is essential to design a system that improves both performance and process control, making it increasingly efficient and secure.

Robust control theory has experienced rapid development with the emergence of powerful tools for the design of control systems. Making possible the control of uncertain systems, and to develope controlled systems with ever better performances. A particular example is the techniques based on Riccati's Algebraic Equations and the

© Springer Nature Switzerland AG 2019
S. Misra et al. (Eds.): ICCSA 2019, LNCS 11620, pp. 731–742, 2019.
https://doi.org/10.1007/978-3-030-24296-1_58

method known as D-K Iteration, which have proved to be very useful in the synthesis of robust controllers H∞ [2, 4–9].

Given the need for improvement in the evaporation systems, this work proposes the design of robust controllers for a system of evaporation of simple effect [2, 6, 10–12]. The modeling and linearization of the study system with respect to a point of operation was performed, additionally, both input and output uncertainties were considered in order to carry out the synthesis of robust controllers. With the design of a control system we tried to keep the system as close as possible to a certain point of operation, mainly we wanted to avoid variations in the density of the product since these affect downstream processes [3, 13, 14].

The paper is organized as follows. Section 2 presents the model of the evaporation process considered. Section 3 presents a controllability analysis of the evaporation process and the controllers synthetized. Section 4 presents some simulation results and Sect. 5 presents the corresponding conclusions.

2 Considered Evaporation Process

The objective of the evaporation system to be controlled is to remove the organic impurities present in the caustic soda (NaOH), the result of its use in previous processes, in order to ensure its reuse in subsequent processes. The first stage of the system consists of a simple effect evaporator where the liquid is processed to achieve a product with a specific density. A simplified diagram of the process is shown in Fig. 1.

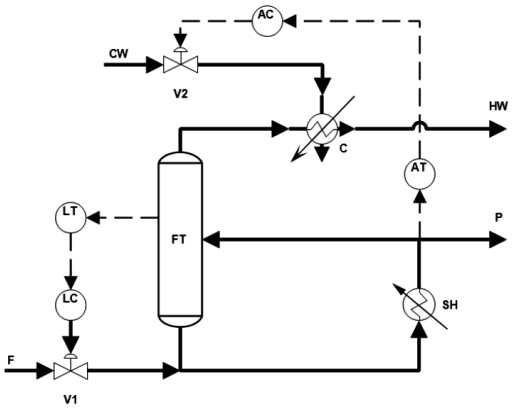


Fig. 1. Simple effect evaporator diagram.

Initially it has the source liquid (SL) to which it is wanted to vary the concentration, later it is passed through steam heaters (SH) in order to achieve a partial evaporation, then part of the liquid coming from the heaters, i.e. the product (P), is used in downstream processes while the rest is sent back to the Flash tank (FT) to be reprocessed. Water vapor escapes through the top of the Flash tank and is condensed (C).

The density of the product and the level of the Flash tank are each controlled by SISO feedback control loops. To control the density of the product ρ_P, the flow of cooling water F_{CW} is manipulated, while the flow of the source liquid F_F is ajusted to maintain a desired level in the Flash tank [1, 13]. The purpose of the control system is to keep the process as close as possible to the selected operating point. It is mainly intended to avoid variations in the density of the product since these affect downstream processes, which in turn constitutes the main source of disturbances in the product flow rate F_P.

2.1 Modeling Considerations

The equations used to describe the system model were obtained from the mass and energy balances in the diagram of Fig. 1. In addition, the following assumptions were made [1, 15]:

- The total volume of liquid in the steam heaters and in the pipe is equivalent to a 23.12 m^2 area tank and 2.21 m height. This volume must be added to the Flash tank.
- The value at which the boiling point of the liquid exceeds that of the water is assumed constant. T_e = 16 °C.
- The difference between the temperature of the hot water and that of the steam to be condensed is assumed to be constant. T_a = 5 °C.
- The temperature of the cooling water is assumed constant T_{RW} = 40 °C.
- The heat capacity of the liquid is assumed constant c_P = 3142 J/kg°C.
- The product density is considered equal to the discharge liquid of the Flash tank $\rho_P = \rho_D$.
- The process is adiabatic and evaporation rates are calculated on the basis of liquid water.
- The volume and mass in the pipes and heaters is kept constant, $F_{FH} = F_{DH}$ and $\rho_{\mathrm{FH}} = \rho_{\mathrm{DH}}$.
- The heat capacity of the source of the heaters and of the discharge is equal to that of the discharge of the Flash tank, $c_{\mathrm{P,FH}} = c_{\mathrm{P,DH}} = c_P$.
- The set-point is assumed to be constant at the corresponding steady-state value.
- Flow ranges are: Source liquid flow $F_F = 0 - 50\,\mathrm{m}^3/\mathrm{h}$ And Coolant Water Flow $F_{RW} = 0 - 700\,\mathrm{m}^3/\mathrm{h}$.
- Initial conditions at steady state: Flow of the source liquid F_F = 25.0147 m^3/h, Coolant water flow F_{WR} = 313.087 m^3/h, Flash tank level $h = 2.71$ m, Flash tank discharge liquid density $\rho_D = 1762\,\mathrm{kg}/\mathrm{m}^3$, Flash tank discharge fluid temperature T_D = 88.431 °C.
- The enthalpy of the vapor escaping from the Flash tank is assumed to be constant $H_V = 2660000\,\mathrm{J}/\mathrm{kg}$.
- Product Flow $F_P = 10\,\mathrm{m}^3/\mathrm{h}$, Heating flow of heaters F_{FH} = 1000 m^3/h and Density of the liquid source $\rho_F = 1300\,\mathrm{kg}/\mathrm{m}^3$.
- The heat capacity of cooling water and hot water are assumed to be constant and equal $c_{P,RW} = c_{P,AH} = 4160$ J/kg °C.

2.2 Model Equations

The dynamics of the model are described by the state equations shown below. Details on obtaining this model can be found in [1, 10, 15].

Flash tank level.

$$\frac{dh}{dt} = \frac{1}{A}(F_F - F_P - \dot{m}_v) \tag{1}$$

Density of the flash tank discharge liquid.

$$\frac{d\rho_D}{dt} = \frac{1}{Ah}\left[\left(\frac{F_{FC} - F_P}{F_{FH}}\right)\rho_F F_F - \dot{m}_v\left((F_{FH} - F_P - \dot{m}_v) - \left(\frac{F_{FC} - F_P}{F_{FH}}\right)(F_{FH} - F_F)\rho_D\right)\right] \tag{2}$$

Flash tank discharge liquid temperature.

$$\begin{aligned}\frac{dT_D}{dt} = \frac{1}{c_P Ah\rho_D}\Bigg[&\frac{(F_{FH} - F_P)(\rho_F F_F + (F_{FH} - F_F)\rho_D)}{F_{FH}} c_P T_{DC} - \dot{m}_v H_v \\ &- c_P T_D\left(\frac{(F_{FH} - F_P)(\rho_F F_F + (F_{FH} - F_F)\rho_D)}{F_{FH}} - \dot{m}_v\right)\Bigg]\end{aligned} \tag{3}$$

Evaporation rate.

$$\dot{m}_v = \frac{c_{PRW}(T_D - T_{RW} - (T_e + T_a))}{(H_v - c_{PRW}(T_D - (T_e + T_a)))} F_{RW} \tag{4}$$

3 Control System Design

This section starts with an analysis procedure named input-output controllability analysis [16], this procedure let us to known if an acceptable control performance can be achieved given a plant. Next, the close loop structure considered in the design and the obtained controllers are presented.

3.1 Model Equations

We present the scaled models for the nominal plant and the representation of the effects of perturbations, according to the procedure developed in [16].

$$\dot{x} = \begin{pmatrix} -0.11677 & 0.070084 & -0.0006847 \\ 17.269 & -45.546 & 0.44493 \\ -38.219 & 0.011099 & -15.798 \end{pmatrix} x + \begin{pmatrix} 0.025032 & -0.017466 & 0 \\ -4.2248 & 11.350 & 0 \\ -0.015751 & -0.0027733 & 315.96 \end{pmatrix} u$$
$$y = \begin{pmatrix} 2 & 0 & 0 \\ 0 & 0.0017794 & 0 \\ 0 & 0 & 0.05 \end{pmatrix} x \tag{5}$$

$$\dot{x}_p = \begin{pmatrix} -0.11677 & 0.070084 & -0.0006847 \\ 17.269 & -45.546 & 0.44493 \\ -38.219 & 0.011099 & -15.798 \end{pmatrix} x_p + \begin{pmatrix} -0.086505 \\ 0.010181 \\ -0.20965 \end{pmatrix} p$$
$$y = \begin{pmatrix} 2 & 0 & 0 \\ 0 & 0.0017794 & 0 \\ 0 & 0 & 0.05 \end{pmatrix} x \tag{6}$$

The input - output controllability analysis of the plant based on the model $y = G(s)u + G_P(s)p$ is performed. Initially, the functional controllability of the G (s) plant is verified, proving that the plant has the same number of inputs and outputs, and that the normal range of G (s) is equal to the number of outputs. It is considered as normal range of G (s) to the range of the matrix G (s) for all values of s, except in a finite number of singularities.

The analysis shows that the first condition is satisfied; the condition of the normal range is equivalent to stating that the minimum singular value of $G(jw)$, $\underline{\sigma}(G)$, must be different from zero (except for those values of jw corresponding to imaginary zeroes).

For the analysis it is required that $\underline{\sigma}(G)$ be as large as possible in the interest frequencies. At frequencies where $\underline{\sigma}(G) < 1$, it is not possible to make changes of magnitude 1 at the outputs using inputs of unit magnitude. It should be noted that since we are working with a scaled model, the maximum variations in the state, input and output variables are of magnitude 1.

Figure 2 shows the singular values of the plant as a function of frequency. The lowest observed singular value is between 1 and 0 (functional controllability) for the frequency range shown. Notwithstanding the fact that the plant has so many inputs and outputs to control, it could lead to difficulties in controlling the nominal plant.

The Relative Gain Arrangement or RGA of a non-singular matrix G is given by $RGA(G) = \Lambda(G) = G \times (G^{-1})^T$. Although this concept was initially introduced as a measure of the interaction of the decentralized control at steady state (ω = 0), the value of the RGA at frequencies close to the cut-off frequency is much more important because it is a good indicator of sensitivity to uncertainty. Therefore, it is difficult to control plants with large elements in the RGA at frequencies close to the cut due to their high sensitivity to uncertainties in the entrances. For the case study when plotting the RGA as a function of frequency it is observed that large values (10^0) are present in the elements of said arrangement which is indicative that the plant is quite sensitive to uncertainties in the inputs (Fig. 3).

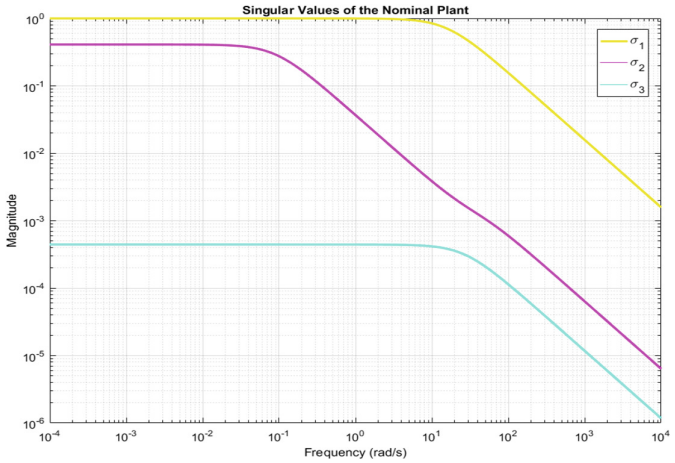


Fig. 2. Singular values of the nominal plant.

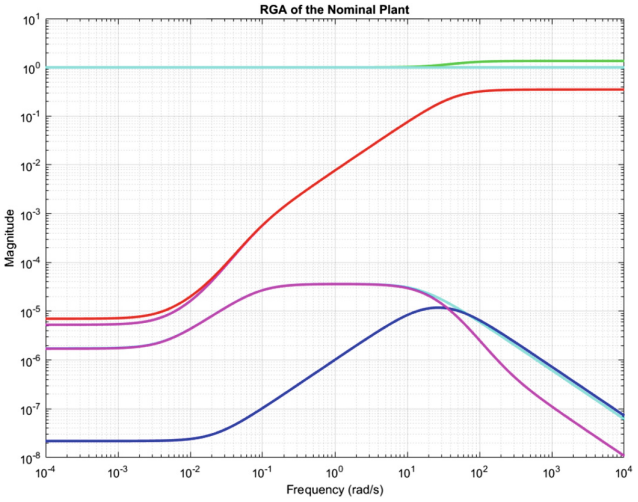


Fig. 3. RGA of the nominal plant

Limitations on system performance are now considered due to restrictions on entries. This is to verify the possibility of achieving a perfect rejection of disturbances by maintaining $|u| \leq 1$. The study system has the form $y = G(s)u + G_P(s)p$; So that to achieve a perfect rejection of disturbances is necessary to do $u = -G^{-1}(s)G_p(s)p$, for the system under study has a single disturbance, so $G_P(s)$ it is a vector. The worst case of the perturbations occurs when $|p(w)| = 1$ and to avoid saturation in the actuators it is necessary to maintain $|u|_{max}$, for which $|u|_{max}$ is required.

Figure 4 shows that for the system being studied, at frequencies lower than 0.1 rad/s a significant control action is necessary. Considering initially the case of

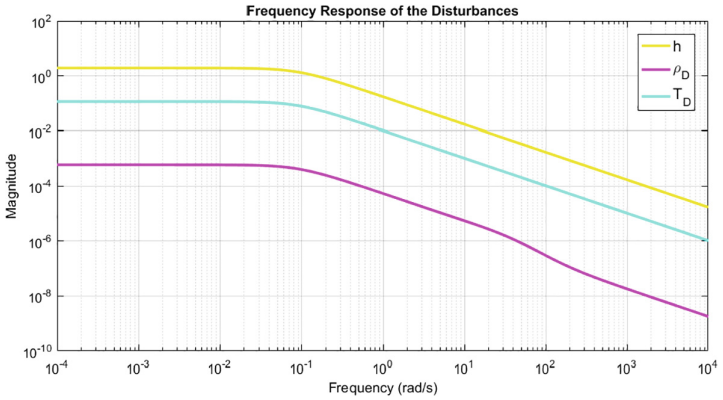


Fig. 4. Frequency response of $G_P(s)$.

control with perfect rejection of disturbances, it is $\left|-G^{-1}(s)G_P(s)\right|_{max}$, therefore it is not possible a total rejection of the perturbations with maximum control inputs unitary as it would cause saturation of the actuators.

Since a perfect rejection of the disturbances is not possible, we consider the problem of verifying if it is possible to achieve an $|e| \leq 1$ error for any $|p| \leq 1$ using $|u| \leq 1$ entries. Each singular value of G, $\sigma_i(G)$ must meet $\sigma_i(G) + 1 \geq \left|u_i^H G_p\right|$ at frequencies where $\left|u_i^H G_p\right| > 1$. Figure 5 shows that the above condition is satisfied at all frequencies.

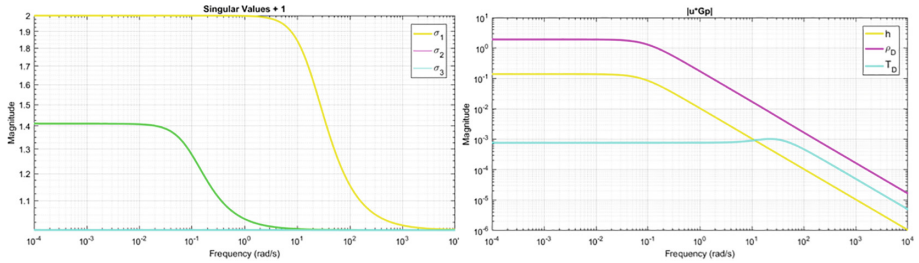


Fig. 5. $\sigma_i(G) + 1$ and $\left|u_i^H G_P\right|$ in frequency

The input - output controllability analysis shows that the system has the following characteristics:

- Although the nominal plant, G (s) is functionally controllable, its minimum singular value is less than 1, which is an indication of possible saturation of the actuators when trying to achieve higher levels of performance.
- The nominal plant presents high sensitivity to input uncertainties (large RGA).
- Although it is not possible to achieve total rejection of disturbances (perfect control), if a steady-state error | e | $\leq$ 1 can be achieved without actuator saturation (acceptable control).

3.2 Controllers

In order to obtain an H_∞ controller, unstructured uncertainties of multiplicative type were considered both in the input and output [16]. Figure 6 shows the block diagram of the system in which, in addition to the uncertainties, both the performance and control signal weights have been included.

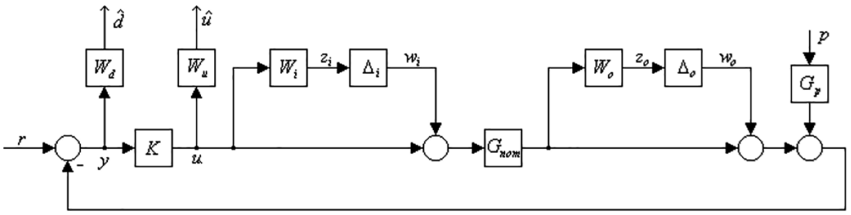


Fig. 6. Block diagram for the closed loop system.

The different weights used for the development of the analysis were:

$$w_i(s) = \frac{0.5077s^2 + 17.46s + 0.6537}{s^2 + 21.36s + 1.354} \qquad w_o(s) = \frac{0.4778s^2 + 7.68s + 0.3835}{s^2 + 11.14s + 0.6792}$$
$$w_d(s) = \frac{0.2s + 1 \times 10^{-5}}{s + 5 \times 10^{-7}} \qquad w_u(s) = \frac{10s + 0.5236}{s + 0.5236} \tag{7}$$

The w_d performance objectives were: achieve a steady-state error of less than 5%, a high frequency amplification of less than 5 dB and a closed loop bandwidth of 1 × 10–5 rad/s. Considering that the rise time of the valves is 60 s, with a minimum attenuation at high frequency of 20 dB and a gain of 1 at low frequency, we chose the weight function of the control signal w_u. Figure 7 shows the block diagram of the system under the M-Δ configuration for the design of robust controllers [4, 16–19]. The controllers obtained are presented below, highlighting that all met the conditions of robust stability and performance.

Controller Obtained by the Riccati Algebraic Equation Solution Method [2, 4, 16–19].

$$K_R(s) = \left[\begin{array}{ccc|ccc} -5e-7 & -3.1e-11 & -3.8e-12 & 2.8e-3 & 4.8e-7 & -1.6e-4 \\ 0 & -5e-7 & 4.6e-14 & 1.6e-4 & 9.6e-7 & 2.7e-3 \\ 0 & 0 & -5e-7 & -4.4e-6 & 2.7e-4 & 5.8e-3 \\ \hline 2.8e-3 & 1.2e-4 & -4.4e-6 & 4e-5 & 9.9e-8 & 2.2e-4 \\ 1.7e-7 & -1.6e-10 & 2.7e-4 & -3.9e-8 & -9.5e-11 & -2.1e-7 \\ -1.1e-4 & 2.7e-3 & 7.4e-8 & -6.9e-4 & -1.7e-6 & -3.7e-3 \end{array}\right] \tag{8}$$

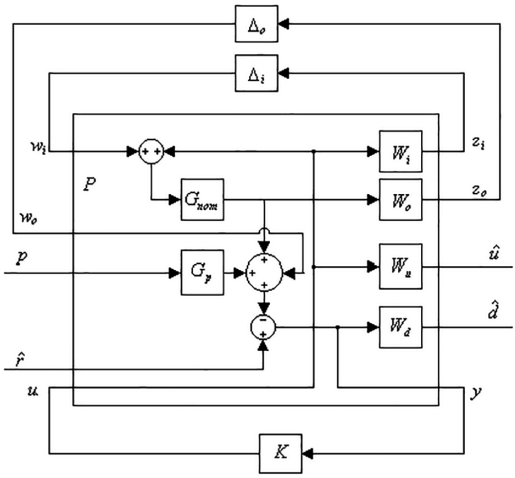


Fig. 7. Configuration for robust controller design

Controller Obtained by the D-K Iteration Method [4, 6, 12, 16]

$$K_{DK}(s)=\left[\begin{array}{ccc|ccc} -5e-7 & 4.9e-10 & 5.7e-12 & 2.6e-3 & 2.2e-7 & -1.5e-4 \\ 0 & -5e-7 & -4.4e-13 & 1.6e-4 & 8.6e-7 & 2.5e-3 \\ 0 & 0 & -7.6e-7 & -2.8e-8 & 2.8e-4 & -7.4e-8 \\ \hline 2.6e-3 & 1.2e-4 & 1e-8 & -2.8e-2 & -3.7e-6 & 9e-5 \\ -2.3e-7 & -3.7e-8 & 2.8e-4 & 2.5e-6 & 3.3e-10 & -7.8e-9 \\ -1e-4 & 2.5e-3 & 2.6e-8 & 4.7e-5 & 6.3e-9 & -1.5e-7 \end{array}\right] \quad (9)$$

4 Results and Analysis

4.1 Results of the Nominal Closed Loop Simulation

The closed-loop gains and the perturbation transfer function were calculated; this is H_∞ norms of the de $[r] \rightarrow \begin{bmatrix} \hat{d} \\ \hat{u} \end{bmatrix}$ and y $[r] \rightarrow \begin{bmatrix} \hat{d} \\ \hat{u} \end{bmatrix}$ transfer functions respectively, in order to compare the performance obtained with the different controllers. See Table 1.

Table 1. Gain of closed loop and disturbances.

Controller	Loop closed	Disturbances
KR	28.285	6.89
KDK	28.28	7.37

Table 2. Value and errors in stationary state of closed loop system outputs

Outputs	KR	KDK
H	1.9–30%	1.96–27.7%
ρD	1779.8–1.01%	1770.3–0.5%
TD	96.4–7.9%	95–7.4%

With both controllers the same gain of closed loop is obtained, however the smaller amplification of the perturbations is obtained with the KR. Table 2 shows the parameters of the steady-state response of the closed-loop system for each controller.

For both cases a large error was obtained in the first output *(h)* (this is because the original system was stable except for the level of the flash tank), achieving the minimum (27.7%) with the K_{DK} controller. With the ρ_D output, an error of less than 5% was achieved in both cases, the minimum (0.5%) was obtained with the K_{DK} controller. For T_D output the smallest error (7.4%) was obtained with the K_{DK} controller.

4.2 Results of Simulation Considering Perturbations in Inputs

We considered a 10% increase in each of the inputs at different time points according to the following data, for h the increase occurs at time $t = 6$ s, for ρD at $t = 7$ s and for T_D at $t = 8$ s. The results obtained for each case were as follows (Table 3).

Table 3. Value and errors in stationary state of closed loop system outputs with input disturbances.

Outputs	KR	KDK
H	1.96–27.7%	2.02–25.5%
ρD	1761–0.06%	1761–0.06%
TD	105–18.7%	104.5–18.2%

The minimum error (25.5%) is obtained on the first output with the K_{DK} controller. For the output ρD, an error of 0.06% was achieved in all cases. For the T_D output a small improvement in the result is obtained with the K_{DK} controller.

4.3 Results of the Simulation Considering Uncertainties in the Parameters of the System

In this case, changes were made in some of the internal parameters of the system such as the feed flow density (ρF of 1300 kg/m^3 to 1250 kg/m^3), the hot water temperature (T_w of 5 °C to 14 °C) of the valves (R from 50 to 100) (Table 4).

For the first output the minimum error (27.7%) is obtained with the K_{DK} controller. While for the output ρD an error of less than 5% was achieved in all cases, the lowest one being obtained with the K_{DK} controller. At T_D output the smallest error (7.4%) was obtained with the K_{DK} controller.

Table 4. Value and errors in stationary state of the uncertainty closed loop system outputs.

Outputs	KR	KDK
H	1.88–30.6%	1.96–27.7%
ρD	1776.6–0.83%	1771.7–0.55%
TD	95.4–7.9%	95–7.4%

5 Conclusion

In this paper, we have presented the design of robust control system for a evaporation process. Two techniques were considered, the first is based in the solution of algebraic Riccati equations and the second is known as D-K iteration method. The performance of the synthetized control systems were verified through simulations. The simulations were implemented using MATLAB®, tool used in this type of work [20], and simulation results show that the controller based on D-K iteration method offers a better performance. The methodology used in this work is applicable to real processes such as shown in [21, 22]. The control systems performance validation through experimental tests will be part of future developments.

References

1. To, L., Tadé, M., Kraetzl, M.: Robust Nonlinear Control of Industrial Evaporation System. World Scientific, Singapore (1999)
2. Lutskaya, N.N., Ladanyuk, A.P.: Problems features of the robust control of process plants. Part II. Examples of modeling of robust control systems. J. Autom. Inf. Sci. **48**(12), 62–69 (2016)
3. Wang, T.-C., Lan, W.-W., Chen, C.-L.: An LMI and fuzzy model approach to H∞ PI controller design. J. Chinese Inst. Eng. Trans. Chinese Inst. Eng. A/Chung-kuo K Ch'eng Hsuch K'an **29**(2), 263–277 (2006)
4. Zhou, K., Doyle, J.C.: Essentials of Robust Control, vol. 104. Prentice Hall, Upper Saddle River (1998)
5. Song, H.K., Shah, S.L., Fisher, D.G.: A self-tuning robust controller. Automatica **22**(5), 521–531 (1986)
6. Huo, L., Qu, C., Li, H.: Robust control of civil structures with parametric uncertainties through D-K iteration. Struct. Des. Tall Spec. Build. **25**(3), 158–176 (2016)
7. Salim, S.N.S., Rahmat, M.F., Faudzi, A.A.M., Ismail, Z.H., Sunar, N.H., Samsudin, S.A.: Robust control strategy for pneumatic drive system via enhanced nonlinear PID controller. Int. J. Electr. Comput. Eng. **4**(5), 658–667 (2014)
8. Bejarano, G., Alfaya, J.A., Ortega, M.G., Rubio, F.R.: Multivariable analysis and H∞ control of a one-stage refrigeration cycle. Appl. Therm. Eng. **91**, 1156–1167 (2015)
9. Darwish, M.K., Al-Gobaisi, Barakzai, A.S., El-Nashar, A.M.: An overview of modern control strategies for optimizing thermal desalination plants. Desalination **84**(1–3), 3–43 (1991)
10. Warren, M., Julian, S., Peter, H.: Operaciones unitarias en ingeniería química, 1199 p (1998)

11. Figueroa, J.L., Agamennoni, O.E., Desages, A.C., Romagnoli, J.A.: Robust multivariable controller design methodology: stability and performance requirements. Chem. Eng. Sci. **46**(5–6), 1299–1310 (1991)
12. Azizi, S.M., Khajehoddin, S.A.: Robust load frequency control in islanded microgrid systems using μ-synthesis and D-K iteration. In: 10th Annual International Systems Conference, SysCon 2016 - Proceedings. School of Technology, Michigan Technological University, Houghton, MI, United States (2016)
13. Stephanopoulos, G.: Chemical Process Control, vol. 2. Prentice Hall, New Jersey (1984)
14. Agamennoni, O., Rotstein, H., Desages, A., Romagnoli, J.A.: Robust controller design methodology for multivariable chemical processes: structured perturbations. Chem. Eng. Sci. **44**(11), 2597–2605 (1989)
15. Holland, C.D.: Fundamentals and modeling of separation processes: absorption, distillation, evaporation and extraction (1975)
16. Skogestad, S., Postlethwaite, I.: Multivariable Feedback Control: Analysis and Design, vol. 2. Wiley, New York (2007)
17. Scherer, C.: Theory of robust control. Delft Univ Technol. (2001)
18. Green, M., Limebeer, D.J.N.: Robust Linear Control. Prentice Hall, Upper Saddle River (1994)
19. Dullerud, G.E., Paganini, F.: A Course in Robust Control Theory: A Convex Approach, vol. 36. Springer, New York (2013)
20. Muñoz, Y., Ospino Castro, A.J., Robles, C., Arizmendi, C.: Implementation of a frequency control in a biomass gasifier system. Int. J. Electr. Comput. Eng. (IJECE) **9**(1), 66–67 (2018)
21. Duarte, J., García, J., Jiménez, J., Sanjuan, M.E., Bula, A., González, J.: Autoignition control in spark-ignition engines using internal model control structure. J. Energy Resour. Technol. **139**(2), 66–77 (2017)
22. Castellanos, H.E., Collazos, C.A., Farfán, J.C., Meléndez-Pertuz, F.: Diseño y Construcción de un Canal Hidráulico de Pendiente Variable. Información Tecnológica **28**(6), 103–114 (2017). https://doi.org/10.4067/S0718-07642017000600012. Accessed 20 July 2018